

The solar wind—its sources, near-sun velocity measurements and acceleration mechanism

S K Alurkar

Physical Research Laboratory, Ahmedabad-380 009, India

Received 25 March 1993, accepted 26 April 1994

Abstract : There have been several reviews on the various aspects of the solar wind phenomenon, its association with the coronal and solar magnetic field structures, and its variation with the sunspot cycle. This overview begins with a brief description of the important findings regarding the solar plasma flow during the last three decades that cover the Skylab and the twin Helios missions.

Besides the long-term studies of the solar wind, sensitive and high resolution instruments in EUV and X-ray wavelengths have made *in situ*, remote and ground-based observations of the sun that have enabled identification of the origins of fast and slow solar winds. Recent high frequency interplanetary scintillation and other radio scattering observations in the transition region are summarized here as they give strong evidence of the acceleration of the solar wind as well as the random motions within about $20 R_{\odot}$ from the sun. Theoretically, extensive evolution of models for coronal heating and solar wind acceleration has resulted in better understanding of the acceleration mechanisms. These will be briefly reviewed to present a consolidated picture of the solar wind phenomena including their origins, velocity structure and association with coronal and magnetic field structures.

Keywords : Solar wind, solar magnetic field, solar wind acceleration

PACS No. : 96.50 Bh.

Plan of the Article

1. Introduction
2. Sources of solar wind
 - 2.1. Coronal holes – sources of steady SW
 - 2.2. Coronal mass ejections (CMEs)
 - 2.3. Coronal streamers
 - 2.4. Other possible sources of SW
3. Acceleration of solar wind – velocity measurements near the sun
4. Acceleration of solar wind – mechanisms of acceleration

5. Conclusions and discussion

5.1. Some important unresolved problems

5.2. Future scope

1. Introduction

The solar (SW) and the heliosphere permeated by it are a result of the primarily thermally-driven coronal expansion ultimately merging into the interstellar medium (ISM). The heat input to the corona may either be steady, as in the case of dissipation of MHD waves or transient when there is a coronal transient or flare. Solar photographs taken during eclipse and *in situ* observations made in the early 1960s indicated the highly structured solar cycle-dependent nature of the solar corona and the consequence of its continuous expansion, the solar wind, Dessler [1].

During the Skylab mission in 1973-74, the coronal holes (CHs) were discovered as the sources of steady high speed streams (HSS), which emanated from these dark coronal regions of weak divergent solar magnetic fields [2-5]. Furthermore, the slow plasma flow was found to be associated with active solar regions comprising bipolar closed loop structures [6-8].

The conceptions regarding the structures of the corona, solar wind and solar magnetic field were based only on these *in situ* observations, which were made at 1 AU and beyond. The large gap of the inner heliosphere (from 0.3 to 1 AU) was bridged by the highly successful mission of the Helios 1 and 2 during 1974-86. The plasma analysers on board made measurements of many important solar wind plasma parameters. This has greatly improved our understanding about the large-scale phenomena of the inner heliosphere including the structure of the solar wind (cf., Schwenn [9]).

The solar magnetic field, which is frozen in the hot, tenuous and highly conducting solar plasma, is dragged into the interplanetary space by the radially outflowing solar wind. The study of the solar wind speed structure, therefore, will be incomplete without the knowledge of the structure of the corona and solar magnetic field. Extensive studies were made of variation of solar wind speed with solar activity cycle for the period 1973-87 using interplanetary scintillation (IPS) method. Kojima and Kakinuma [10] reported distribution of low- and high-speed regions on the source surface over the solar cycle. In a similar study Rickett and Coles [11] compared IPS speeds with coronal density and solar magnetic field. They confirmed the Skylab finding of the strong association between high-speed streams and open-field, low-density CHs on one hand and between slow plasma flow and denser coronal regions, comprising K-coronal white-light in a narrow band around the solar equator, also Alurkar *et al* [12], on the other.

The study of the development of CHs and their variations over a solar cycle, using the Mauna Loa K-coronameter white-light observations made during 1965-78, showed disappearance and reappearance from poles of large CHs at solar maximum and minimum respectively, Hundhausen *et al*, [13]. Extensive analyses of the behaviour of the heliospheric

current sheet (HCS) over the solar cycle 21 were made by applying a current-free “potential field model” to the measured line of sight component of the photospheric magnetic field [14,15].

Besides the long-term studies of solar wind and related coronal phenomena mentioned above, there have been several studies regarding solar wind-related specific topics, such as coronal heating, acceleration of solar wind [16–20] and interplanetary turbulence [21–25] which have substantially improved our understanding of the solar wind phenomenon as a whole.

The objective is to assemble together the important aspects of the solar wind, such as its origin, velocity structure, association with solar magnetic field and coronal structures, variation with solar activity cycle, *etc.* The present thinking about the solar wind acceleration mechanisms as also of generation of slow and fast wind will be presented. The overview will be concluded with a brief discussion of the scope, if any, for future work.

2. Sources of solar wind

At least three source regions of solar wind have been identified—coronal holes, coronal streamers (and/or sector boundaries) and coronal mass ejections (CMEs). These sources occupy nearly half of the solar surface area. The rest of the area, forming the ‘quiet’ coronal region of medium X-ray brightness on the photosphere (Figure 1) showing soft X-ray photograph of the Sun), is the source region of the solar wind that is responsible for about 50% of the total mass loss from the Sun, Bird and Edenhofer [26].

The contribution of other coronal features, like upward moving spicules, macrospicules and high-speed jets in the transition region, to the solar wind is still a conjecture, Brueckner and Bartoe [27].

2.1. Coronal holes—sources of steady SW :

Observations of the inner corona ($3-9 R_{\odot}$) or the *K*-corona, wherein the Thompson scattering of the photospheric light by free electrons occurs, were made using a *K*-coronagraph on board the OSO-7 spacecraft in early 1970s by Howard and Koomen [28]. A good correlation was found between the enhanced brightness (and therefore enhanced electron density) of white-light, coronal streamers and the structure of interplanetary magnetic sectors. Close to the sun the heliospheric current sheet (HCS) warping, caused by the underlying sectors, can be large. The network of closed field lines below the HCS traps the plasma, thereby enhancing the density and brightening the white-light corona.

In contrast, away from the sun the corona is dark during quiet conditions. Such coronal regions, with low brightness and low density, are known as “coronal holes”. These are cool, large regions with weak and mainly unipolar magnetic fields which extend away from the sun in divergent open field lines. High speed plasma streams gush out from the CHs and, on encountering the magnetosphere of the earth, cause geomagnetic storms.

In 1973 (descending phase of solar activity cycle) one recurrent HSS, when mapped back to the sun, was found to originate in an equatorial CH [2]. This association between CHs and HSS was confirmed during the OSO-7 and Skylab observations [29, 30].

The coronal holes were confirmed as source regions of long-lived fast solar wind streams during the Skylab mission in 1973-74. They were found to be located over open field line regions, such as those at the polar caps during solar minimum [5]. The slow SW, on the other hand, originated from above more active regions on the Sun, where sunspots, solar flares and eruptive prominences predominate and are associated with 'closed' magnetic field structures, coronal streamers, *etc.*

The Skylab observations also confirmed that the SW speed is always down to about 300 km/s at any neutral line or sector boundary. Speeds of about 740 km/s occur beyond some distance normal to any neutral line. The occurrence of fast and slow wind was also interpreted as having large spatial gradients, of 50 km/s per degree of heliographic angle, in the SW, Svalgaard and Wilcox [31].

It was found that, except at the solar maximum when CHs disappear from the solar poles, CHs exist at the poles almost throughout a solar cycle, and therefore HSS were expected to originate in the polar coronal regions, Withbroe *et al* [32]. This suggestion was consistent with the findings of Rickett and Coles [33], who studied the variation of solar wind speed structure, measured by the method of interplanetary scintillation, over a solar cycle during 1971-82. They showed that fast wind (faster than 500 km/s) originated in regions beyond $\pm 30^\circ$ heliolatitudes, whereas slower wind emanated from lower latitudes throughout the solar cycle, with its extension to high latitudes around solar maximum.

The Skylab finding that HSS originate in CHs [4] was explained in an interesting way by Levine *et al*, [34]. They established a physical relation between the interplanetary magnetic field (IMF) and SW measured at the earth and their sources on a spherical sources surface at $2.5 R_{\odot}$ from the Sun. The open magnetic field lines, which extend from the photosphere into the interplanetary space, are traced in the potential field (no coronal currents) approximation to the large-scale field using measured line-of-sight component of the photospheric magnetic field as a boundary condition, Altschuler and Newkirk [35]. This method of calculating the coronal magnetic pattern is very simple. Significant differences between the estimated global magnetic field pattern and the potential field configuration at the photosphere may be detected only when coronal electric currents have magnitudes in excess of 30% of those of the large-scale photospheric currents [34]. In Figure 2 (upper portion) only magnetic field lines extending into the space are shown. Their footpoints coincide with the positions of CHs determined from X-ray data (lower portion). Levine *et al* found an inverse relation between SW speed measured at 1 AU and the expansion rate of the coronal field. The latter is defined as the ratio of field strengths $B(R_s)/B(R_S)$ where $B(R_s)$ is the field strength at a point P on the equator at a source surface of radius R_s . $B(R_S)$ is the field strength at the end of a field line joining P with the photosphere. This ratio gives the relative area covered by a flux tube. A further confirmation of the Skylab finding that large CHs are the coronal regions of HSS observed at 1 AU was reported by Lindblad [36]. He carried out an extensive correlation



Figure 1. Soft X-ray photograph of the corona in 1973 showing : *coronal holes* (dark areas) near east limb at left and poles. *Active regions* (large bright areas) and coronal bright points. *Quiet regions* (medium bright areas); Withbroe [16].

analysis between individual high-speed streams observed by near-earth spacecraft during the period 1971-74 and specific CHs identified on *K*-coronal isophotal maps of the white-light corona. Figure 3 is based on 88 SW stream-polar CH associations and 14 SW stream-equatorial CH associations. The inferred source longitude of peak velocity of each HSS is plotted against the observed Carrington longitude of maximum equatorward extension of CH.

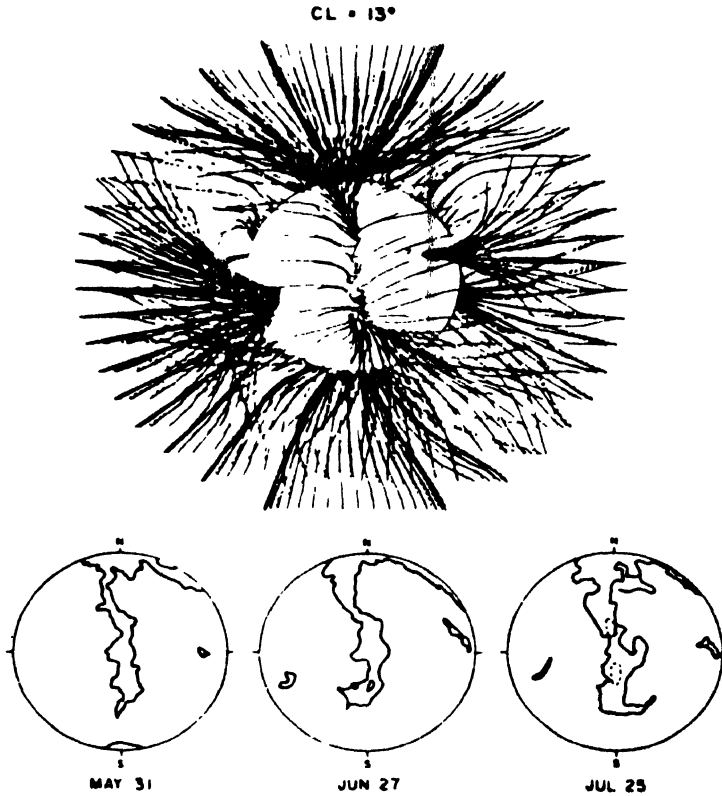


Figure 2. Open field line coronal regions estimated from measured photospheric magnetic fields and corresponding contour maps showing locations of coronal holes Levine *et al* [34]

The 45°-line through the data points showed a perfect agreement between the computed locations of the sources of peak velocity and those of the equatorward tips of polar CHs.

The correlation between CHs, the *K*-coronal white-light band, encompassing streamers and closed magnetic loop structures, and solar wind speed was studied by Hundhausen [37]. The upper part of Figure 4 shows a synoptic map of white-light brightness measured at 1.5 R_{\odot} for Carrington rotation 1616 and polar CHs, with appropriate magnetic polarities, extending down to the solar equator. The bright corona is marked by the winding contours of the *K*-corona intensity. This band has two sectors. The lower part shows observed SW speeds with the corresponding magnetic polarity. Two streams of speeds of 800 km/s are seen to originate in two CHs with similar polarities. The slow wind with speeds

of 400 km/s or less, on the other hand is seen to have originated in the bright white-light band.

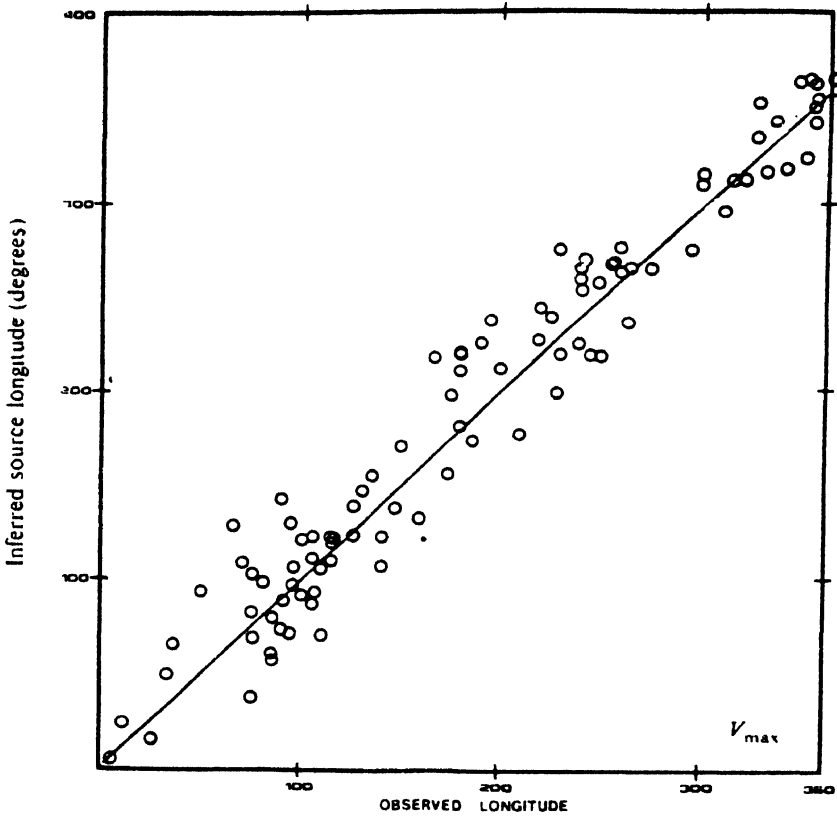


Figure 3. Inferred solar source longitude of maximum velocity of high-speed streams versus Carrington longitude of maximum equatorward extension of coronal holes for 102 coronal hole – solar wind stream associations Lindblad [36].

2.2. Coronal mass ejections (CMEs) :

This is one of the most extensively observed coronal phenomena by coronagraphs on board spacecraft since 1970s and by a ground-based coronameter since 1980s. Although CMEs are established as coronal sources of solar wind, they account for a mere 5% of the total solar mass loss by the SW. Various aspects of this regularly observed phenomenon have been reviewed by several authors [26,38–42]. Some pertinent characteristics of CMEs are summarized below :

In 1973-74 the Skylab observations showed ‘coincident’ association between CMEs and eruptive prominences and chromospheric flares [43,44]. Long-duration soft X-ray also accompanied the eruptive prominences, and therefore were thought to be associated with CMEs [45,46]. The development and acceleration of CMEs were earlier explained on the basis of these associations. These ideas have now been completely revised due to the

observations of formation of typical structures in a few cases of CMEs and more accurate studies of temporal and spatial associations between flares and CMEs. It is now believed that both types of chromospheric activities, eruptive prominences and flares, are a result, rather

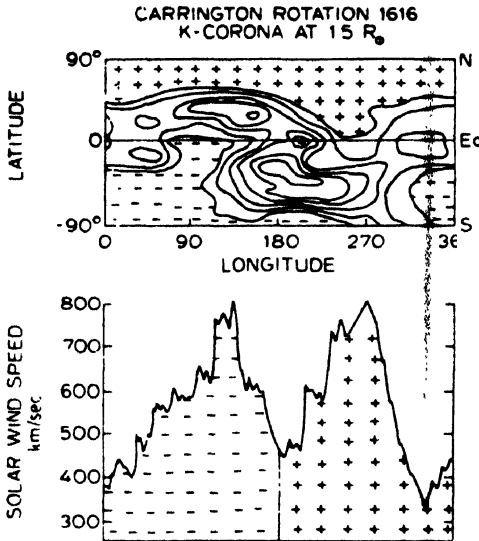


Figure 4. Contour map of K-coronal brightness in 1974 and measured solar wind speed and magnetic polarity variations with inferred Carrington source longitude. The two high-speed streams are assumed to originate in solar regions marked by the same polarity as the stream Hundhausen [37].

than a cause, of a global magnetic field change which causes the mass ejection [42]. Briefly, Hundhausen [37] compared the formation of a bright loop, observed in a CME, through deformation and compression of the background plasma to the formation of a bow shock in a fluid, provided the upward motion of the cavity is both super-Alfvenic and supersonic or both sub-Alfvenic and subsonic. The former results into a bow shock, while in the later a gradual deformation of the background magnetized plasma occurs. The motion in many CMEs has been inferred to be sub-Alfvenic and supersonic. A shock, formed in this interaction may move at the speed equal to that of the body (the cavity), and therefore be sub-Alfvenic. Following this explanation, it was suggested that ‘slow MHD shock’ might occur at the front of a CME with sub-Alfvenic but supersonic speed, Hundhausen *et al* [47]. This unusual scenario, without a parallel in fluid mechanics, is yet to be accepted widely.

At solar maximum the rate of occurrence of CMEs is 1 or 2 per day, which slows down to 1 per week [40,48]. Their speed lies between 200 and 1000 km/s.

2.3. Coronal streamers :

The contribution to solar wind from these coronal features comes in the form of slow SW in the sector boundaries. Brighter than the background coronal intensity, these helmet-like elongated structures emerge from above active regions associated with closed magnetic loop

systems. Coronal streamers extend beyond $2 R_{\odot}$, sometimes upto $10 R_{\odot}$, as inferred from eclipse photographs, Withbroe [49]. Unlike in the case of CHs and CMEs, the real contribution of streamers to SW is unknown Figure 5. The polarity reversal, shown in this

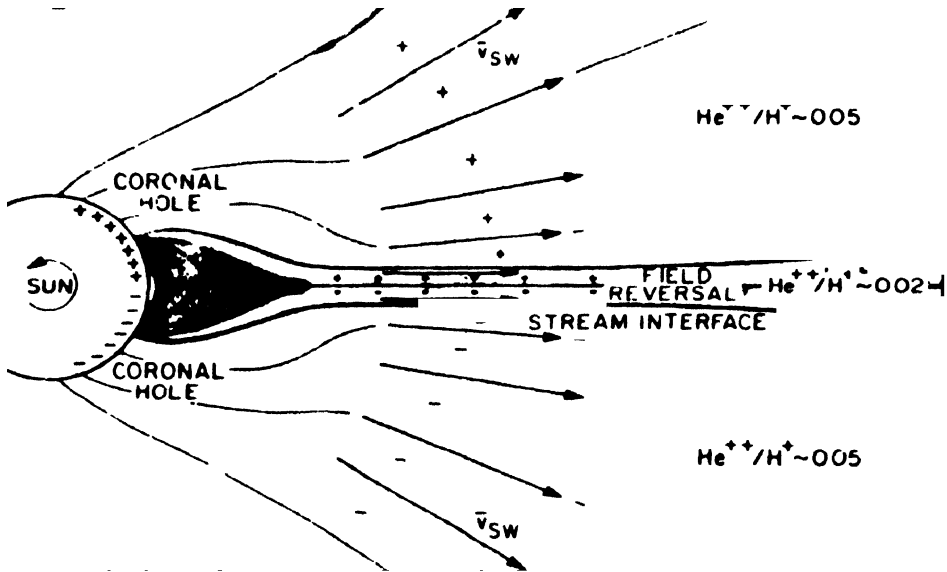


Figure 5. Idealized schematic view of an equatorial streamer. Gosling *et al* [50]. Plasma within the streamer is denser, flows slower and has a lower helium abundance than that outside the streamer.

model, Gosling *et al* [50], for streamers and their interface with CHs, is known to trace back to a coronal streamer; this interface coincides with a sector boundary. The latter are regions with slow speed wind, high proton density and low helium abundance [50] (Figure 6).

2.4. Other possible sources of SW :

CHs, CMEs and streamers are well-studied and identified as sources of solar wind. There is a whole class of micro-scale coronal features which are suspected to contribute to the outflow of the solar mass. Polar plumes, X-ray bright points and spicules fall in this category, Ahmad and Withbroe [51].

Very high resolution UV observations of the Sun have discovered short-lived high speed plasma jets which might accelerate the solar wind. These energetic phenomena are observed in spectral lines in the transition region ($T \sim 10^5$ K) and move with typical speeds of ~ 400 km/s. [27]. The origin of fast SW in some of these fine-scale coronal phenomena is in the form of 'microflare activity' in supergranular convection, Axford and McKenzie [19]. Being too small in scale-size to be observable with the presently available spatial resolution, their detailed studies are not possible. The only advantage is that the microflare activity manifests itself in high-speed plasma jets and X-ray bright points.

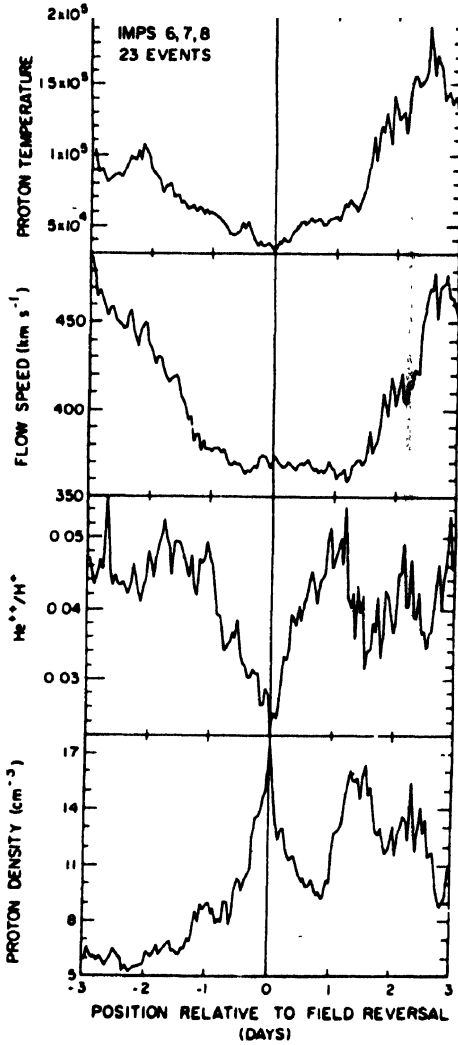


Figure 6. Superposed epoch plots of solar wind proton density, helium abundance, flow speed and proton temperature for 23 well-defined sector boundaries more than 1 day away from speed enhancements associated with high-speed streams. 1-hour averages are used, and sector boundary passage was used as zero epoch. The data were collected at 1 AU from the IMP 6/7/8 spacecraft, Schwenn [9].

3. Acceleration of solar wind-velocity measurements near the sun

In situ and remote measurements by spacecraft and ground-based observations by the interplanetary scintillation (IPS) technique have provided a wealth of data on solar wind bulk velocity within about $15 R_{\odot}$ from the sun. This essentially covers the transition region wherein most of the solar wind acceleration occurs. Ideally, the radial variation of the solar wind bulk velocity can be studied by using a series of plasma probes along a radial direction. Helios 1 and 2 almost satisfied this arrangement when they made statistical observations of the

solar wind bulk velocity in the ecliptic plane. It was found that the acceleration to the maximum velocity was nearly complete within 0.3 AU, the closest approach of the spacecraft to the sun [9,26]. It thus became apparent to measure the radial dependence of solar wind velocity within this distance for understanding the acceleration mechanisms.

EUV measurements of Doppler shifts of emission lines in the transition and coronal regions and spaced-telescope IPS technique are the main methods for estimating the bulk velocity of the solar plasma flow that fall in the category of remote observations. Whereas the EUV technique can measure the bulk velocity at different heights along a radial direction in the acceleration region, the IPS yields temporal and spatial average flow speeds. The latter has, however, measured speeds covering the whole range from the turbulent velocities near the sun to the asymptotic ones 1 AU and beyond

In an extensive review of the coronal transient phenomena the importance of the background solar wind close to the Sun has been emphasised [38 and references therein]. Spacecraft observations show a velocity increase from ≤ 100 km/s within $15 R_{\odot}$ to ≥ 200 km/s beyond this distance. EUV observation of regions within coronal holes and transition region [52,53] indicated flow speeds from 3-5 km/s in the transition region to 85 km/s near $4 R_{\odot}$. This acceleration region was described as a 'turbulent envelope' around the sun [54,56].

These velocity observations close to the Sun, indicating acceleration of the solar plasma flow in the transition region with the steep temperature gradient, are consistent with those predicted by Parker [57,58] in his thermally-driven isothermal model for the continuously expanding solar corona. The relevance of the buoyance effect of this background solar wind near the sun of the CMEs has been emphasised by Dryer in his review [38]. According to him, the background of the turbulent envelope near the sun is relevant to the triggering of the coronal transients at the sun and their propagation through the interplanetary medium. Ultimately, their manifestations as shock waves are detected by spacecraft and IPS 'g-map' technique Hewish *et al* [59].

Since early 70s, radio telemetry links between the earth and a spacecraft located near superior conjunction have been used to study the dynamics of the lower solar corona, including the acceleration region of the solar wind. Details of five different radio source studies of the solar corona yielding measurements of electron density, magnetic field, perpendicular component of solar wind velocity and wavenumber spectrum of density fluctuations have been lucidly explained in a review on coronal investigations with occulted spacecraft radio signals by Bird [60].

An important measurement of the plasma flow velocity at $1.7 R_{\odot}$ from the sun was made by Woo [61] at 2.3 GHz on Helios 1 and at $1.3 R_{\odot}$ at 8.4 GHz on Viking Tyler [62] using the phenomenon of spectral/angular broadening. This results when radio waves, which are scattered by the inhomogeneities of refractive index in the coronal plasma, broaden their

signal in frequency and apparent angular size. Since variations in refractive index are proportional to those in the electron density ($n = 1 - 40.3 \frac{N}{f^2}$), these broadening effects depend on the coronal turbulence [60].

Woo [61] has shown that the perpendicular component of the bulk velocity of the plasma flow is given by

$$V_{\perp} = \text{const} \cdot \frac{1}{f} \frac{\Delta f}{d\theta} L,$$

where the constant is independent of coronal turbulence

Δf = frequency broadening

$d\theta$ = angular broadening

$L = \frac{\rho}{\rho - \cos \epsilon}$, ρ = distance of spacecraft from earth in Au,

ϵ = solar elongation angle and

f = signal frequency.

Thus, using this formula, simultaneous measurements of spectral and angular broadening of a monochromatic signal can lead to v_{\perp} , Woo *et al* [63]. Woo [61] made the first measurement of $v_{\perp} = 24$ km/s at $1.7 R_{\odot}$.

An important observation that is relevant to the understanding of the solar wind acceleration phenomenon is radio occultation probing of the 'transonic region' from subsonic to supersonic plasma flow near the Sun. Scintillation studies of compact water vapour masers have observed enhanced scintillations in the region lying between radial distances of 10 and $20 R_{\odot}$. This scintillation enhancement is consistent with the Helios observations of radial variation of scintillation index m of S-band signal strength. The enhancement was detected in the radial range $10-25 R_{\odot}$, relative to the radial power-law fit of $m(R) \propto R^{-1.55}$, which was interpreted in terms of Alfvén wave mode dissipation beyond the supersonic distance. Armand *et al* [64] confirmed this by spacecraft observations. This energy input accelerates the solar wind plasma flow beyond the asymptotic speed. This region is identified with the transonic region [65 and references therein]. The necessity for these observations became obvious when the radial solar wind velocity profiles derived from radio occultation techniques were compared with that of the hydrodynamic model for solar wind by Parker [57]. In Figure 7 [65], curves 1 to 3 show the average radial velocity profiles, v_{eff} , compared with the Parker's velocity profile, Curve 5. Curve 4 gives the velocity profile of sound. Whereas the Parker's model yields a monotonically increasing velocity profile, the empirical velocity profiles indicate a steep rise of v_{eff} in the transonic zone lying in the range $8-25 R_{\odot}$.

Figure 8 [65] shows that the rms deviations of flow velocity, σ_v [55,66] and the enhancement in scintillations [67,68] take place at the transition to the supersonic flow. Although the sharp rise in σ_v and the anisotropy of scattering of radio waves (derived from

observations of occultation of Crab Nebula by the solar corona) in the region $10\text{--}20 R_{\odot}$ were known earlier [54,69], their relevance to the transition from the subsonic to the supersonic flow was realized nearly a decade later.

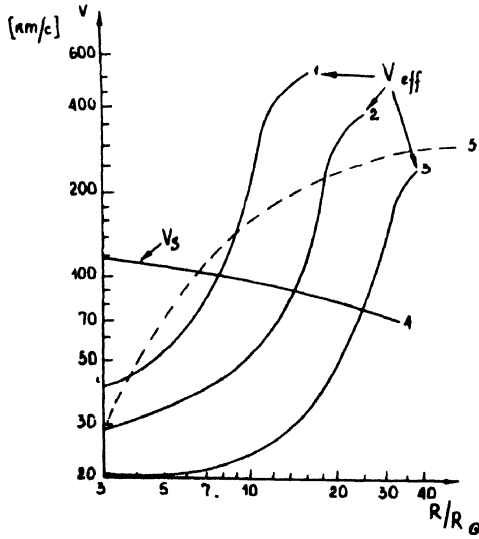


Figure 7. Measured radial dependence of solar wind velocity; (1) 1977 data Armstrong and Woo [55]; (2) 1975 data; (3) 1976 data Yokovlev *et al* [82]; (4) Sonic velocity, v_s ; (5) dashed curve-Parker's hydrodynamic model for solar wind, [65].

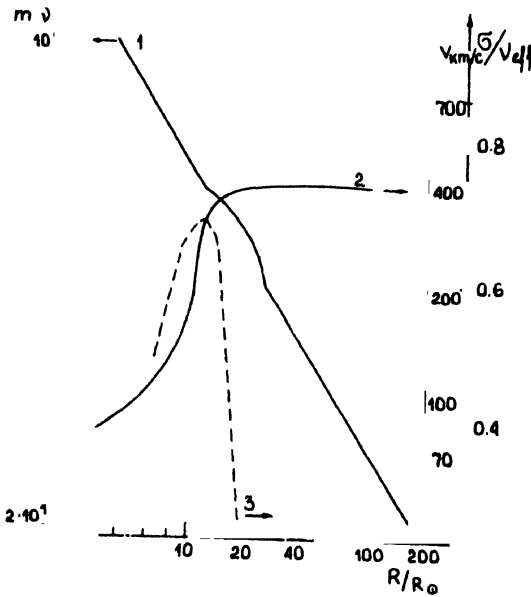


Figure 8. Radial variation of scintillation index \times operation frequency, mv (curve 1), typical solar wind velocity (curve 2), and fractional solar wind velocity (curve 3), [55,65].

Several physical parameters of the plasma medium in the transonic region, which include scintillation index, source and spectral broadening, radial profile of bulk velocity,

random velocity σ_v , along the line of sight, radial variation of turbulence (ΔN_e), show enhancements in the radial distance range 10–12 R_\odot . This range also includes the region wherein solar wind acceleration of 5–9 km/s² has been estimated from observations of Doppler shifts of transition region and coronal emission lines on the photosphere, Rottman and Orrall [70].

The main features of the radial variations of these parameters are explained by assuming the transonic regime ($R \simeq 10\text{--}25 R_\odot$) as a mixed-flow region comprising the subsonic and supersonic plasma flows [65]. This assumption is based on the stream structure of the two flows, in the form of stationary large-scale velocity distribution, which was represented by a velocity distribution function. The observed variation of the latter in the supersonic flow regime explains the observed radial variation of the random velocity component (σ_v), which is one of the most important parameters of the transonic plasma flow.

In this connection it is very important to recall the observations of the random component of the flow velocities, centered around 15 R_\odot to form the 'turbulent envelope' [54]. It is at this radial distance that the sharp change in the σ_v profile occurs (Figure 8). This is suggestive of a selective type of wave damping, particularly that of the Alfvén mode MHD waves, similar to that associated with the steep temperature gradient in the transition region.

Intensity scintillation spectra were estimated at cm wavelengths in the solar radial distance range 5–100 R_\odot . The power-law spectral shape changed steadily in the near-sun region. This was attributed to systematic variations in the important parameters of the plasma medium, particularly, the mean velocity, random velocity, microturbulence spectrum and the spatial anisotropy [66]. They observed high random velocities inside of 30 R_\odot , a region which includes the solar wind acceleration regime. Scott *et al* [66] suggested that the random velocities could be due to some wave action, particularly of Alfvénic mode MHD waves, in the electron density spectrum, with radial velocities of ± 250 km/s.

Using the IPS method with the VLA-telescope, the solar wind acceleration region between 3 and 12 R_\odot was observed, Kojima *et al* [71]. The random velocities known to be observed in this region by IPS are attributed to MHD wave motions, which are responsible for accelerating the solar wind even beyond the asymptotic velocities. They observed a sudden change in velocity in the range 3–4.5 R_\odot . This seems to be consistent with the rising part of the random velocity profile $\sigma_v(R)$ in Figure 8.

In an overview of SW velocity measurements inside of 0.3 AU from the sun and their comparison with theoretical coronal velocity profiles, data of four different radio sounding techniques were considered [26 and references therein]. They are : (i) Multistation intensity correlation measurements; essentially IPS of radio sources; (ii) Phase scintillations of a spacecraft signal; (iii) Spectral and angular broadening of a spacecraft signal; and (iv) estimation of a Fresnel frequency in the power spectrum of intensity scintillations. Bulk velocities estimated by the IPS technique had compared well with the *in situ* measurements made by interplanetary spacecraft, Coles [72]. This study encouraged to employ this method to make SW velocity measurements within 0.3 AU.

Although the data used in this overview [26] were taken at many different heliolatitudes and during different phases of sunspot cycle, some broad conclusions were drawn : (i) All the velocity values were smaller than those expected for a large polar CH. (ii) Most of the velocity values lie between two computed velocity profiles for SW with and without an additional MHD-wave energy input. (i) follows from the fact that the polar CH was assumed to have a fast diverging magnetic line configuration which, as in observed, gives out a fast plasma flow. (ii) is consistent with the SW acceleration mechanisms discussed in Section 4.

4. Acceleration of solar wind – mechanisms of acceleration

For the continuous expansion of the corona to the flow speeds of streams observed at 1 AU, one has to consider the force balance in the corona, the solar wind mass flux and the energy balance. It is well known that the primarily thermally-driven model of the solar wind [57] accounts for the first two quantities satisfactorily, but not for the energy balance. As a result, the flow speeds given by this model fall short of the values of the high speed streams (≥ 600 km/s) observed at the earth.

However, the problem of the energy source for the coronal expansion is connected with that of the coronal heating which is not yet fully understood. Since the photosphere is cooler by about three orders of magnitude than the corona, it is necessary to first transport an appropriate form of energy from the photosphere to the corona. It is suggested that the fluctuations in the convection zone carry this energy to the corona, where it is added on to the thermal flow energy of plasma, Holzer [73]. Presently, it is thought that MHD waves, which are least damped, transport this energy to the corona, which in turn is supplied by two sources : thermal conduction from the million degree corona, and the part of the MHD wave flux which is believed to heat the corona.

Studies of the thermally-driven solar wind models showed that for normal values of coronal density and temperature, the speed of the solar wind emanating from coronal holes is much lower than that observed in high-speed streams at 1 AU [74]. Interestingly, adding energy in the subsonic region (within $5 R_{\odot}$) resulted in large mass flux but lower asymptotic velocities, and energy addition in the supersonic region ($5-10 R_{\odot}$) yielded higher asymptotic velocities without changing the mass flux [75]. Hollweg [76] also has suggested that the Alfvén waves from the lower corona can accelerate the solar wind.

It is known that the highly divergent magnetic flux tube configuration of coronal holes results in low plasma density. If the damping length of the mechanical energy flux is inversely proportional to the coronal density, the dissipation of the MHD waves and their energy transfer to the solar wind will be distributed over larger coronal distances, beyond the sonic point. On the other hand, the same input energy flux into less divergent magnetic flux tubes would dissipate mainly inside the sonic point. This distribution of energy deposition is capable of producing the high velocity streams in coronal holes as also the higher mass flux observed in the slow-speed solar wind [16,23].

Munro and Jackson [77] showed that an average energy flux density of $(4 \times 10^5 \text{ ergs cm}^{-2} \text{ sec}^{-1})$ derived from the coronal base must be added to the thermally-driven flow from a coronal hole with a magnetic flux tube expansion factor of 7.2 in order to accelerate it. Alfvén waves with amplitude of 20–30 km/s can carry this energy flux.

Parker [17] has discussed a special form of heat input for producing fast streams in solar wind from coronal holes. More than half the heat $(\sim 3\text{--}4 \times 10^5 \text{ ergs cm}^{-2} \text{ sec}^{-1})$ is supplied to the coronal hole near the sun $(R \leq 3 R_{\odot})$ and an additional heat input $(1\text{--}2 \times 10^5 \text{ ergs cm}^{-2} \text{ sec}^{-1})$ beyond the sonic point $(R \geq 5 R_{\odot})$. The former can come only from plasma jets, fast particles and short period ($\leq 10 \text{ sec}$) MHD waves from the network activity. The latter energy flux can come only from the dissipation by thermal conduction of long period ($\geq 10^2 \text{ sec}$) MHD waves from the convection below the photosphere.

It is known that open field line structures occur in weak-field regions, and mainly in the regions from where the field lines extend to low field densities. The steady fast (500–800 km/s) as well as the steady slow (400 km/s) wind emerge from these open field regions, Parker [78]. This assumption of a common source for the fast and slow winds is rather difficult to justify as they have several parameters with different values : *e.g.* (i) proton density, which is 3.6 times larger in the slow wind than that in the fast; (ii) helium-to-proton ratios in the fast and slow wind are 3.6% and 2.5% respectively beyond 0.5 AU; [9 and references therein] and (iii) the fast wind is often accompanied by the Alfvénic turbulence. There is a strong correlation between the fluctuations of bulk radial velocity and those of the magnetic field vector [79,80]. Thus, the two states of solar wind are of different nature and, therefore, they may have their own specific generation/acceleration mechanisms. However, the CHs are strongly influenced by the solar activity cycle. How could then the separate identity of the two solar wind states be maintained?

An alternative mechanism for generating HSS is in the form of 'micro-flare activity' in supergranular convection [19]. The interplanetary magnetic field (IMF) is anchored in a network of magnetic field lines forming the boundaries of the chromospheric supergranulation. A bidirectional field results due to the continual addition of flux at the sides of the slow, super-Alfvénic, upwelling flow at the center of the supergranulation that spreads horizontally, subsequently cooling and flowing down at the edges where the network is formed. Supergranulations last for a day or two and are about 30,000 km across, with a horizontal speed of about 1 km/s. The energy necessary to accelerate the SW is available in the network and is extracted from the convection in the supergranulation. This energy is converted into magnetic energy which, in turn, is converted into intense hydromagnetic activity due to 'microflares'. The latter are associated with magnetic field reversals in the not strictly a unipolar network.

The problem with the microflare activity is that it is too small in scale-size to be observable with the existing spatial resolution. Even so, it manifests itself as plasma jets and X-ray bright points.

There are unsolved problems with the slow SW too. During solar minimum, this wind (≤ 400 km/s) is found to be associated with the near-equatorial, narrow ($\pm 20^\circ$ of the equator) belt of K -coronal white-light intensity and coronal streamers. This is also band lying above active regions with closed-loop magnetic structures, and with heliospheric current sheet (HCS) attached to the equator, Schwenn [81]. In contrast, during solar maximum, the slow plasma flow regions extend to higher heliolatitudes and this wind emanates from larger coronal areas [10–12] remote from the HCS and coronal streamers. It is not quite clear how the transformation from the closed-loop systems in the lower corona to open field line structures takes place by the outflowing slow flow.

5. Conclusions and discussion

Due to the highly successful space missions of the Skylab and the twin Helios, our understanding of the solar wind phenomenon in the inner heliosphere (between 0.3 and 1 AU) has improved considerably. It was confirmed that the high-speed streams (HSS) originate in the coronal holes (CHs). The weak and highly divergent magnetic field of the CHs is thought to be responsible for the fast streams. The slow plasma flow, in contrast, emanates from denser, active coronal regions with bipolar magnetic loop systems over which coronal streamers lie. The associated areal expansion rates of magnetic flux tubes have shown inverse relation with the solar wind flow speed.

CHs were found to be strongly influenced by the solar cycle. They disappear from the poles at solar maximum and reappear at minimum. On application of a current-free potential field model to the photospheric magnetic field, the warping of the heliospheric current sheet (HCS) showed its strong association with the solar cycle. During a solar minimum, the flat HCS nearly coincides with the equatorial plane, while during a maximum the excursion of the warps reaches 15° – 20° heliolatitudes. This has enabled high latitude measurements of flow speed and other parameters.

Remote sensing Doppler shifts of EUV emission lines and velocity measurements by IPS and other radio scattering techniques in the transition region have been used to study the acceleration of the solar wind. It was observed that the solar wind acceleration occurred in the region 3 – $12 R_\odot$ from the sun. The random velocity component, which forms a 'turbulent envelop' around the sun in the region, is attributed to some kind of wave action in the form of MHD waves.

The present status of the theoretical development regarding coronal heating, SW acceleration and interplanetary turbulence is briefly discussed. Parker's hydrodynamic model for thermally-driven SW, yields asymptotic flow speeds at 1AU of about 600 km/s or less, much lower than those observed in fast streams. Since the photosphere is much cooler than the corona, it is necessary to first transport an appropriate form of energy from the photosphere to the corona. The least damped MHD waves, particularly the Alfvén waves, are thought to transport this energy to the corona. Recently, Parker [17] has suggested a unique process of producing high speed streams from CHs, involving a two-stage heat input in the

corona. In the first stage, more than half the heat is supplied to the base of a CH, and an additional heat input is provided at the sonic point.

The micro-flare activity in supergranular convection has also been suggested as a possible mechanism for generating HSS from CHs [19]. But its small scale-size prohibits its detection.

An unambiguous generation mechanism for the slow SW is also not yet known. During solar minimum, this wind is strongly associated with the near-equatorial $\pm 20^\circ$ wide belt of *K*-coronal white-light intensity and coronal streamers. But during solar minimum large regions of slow wind appear at high heliolatitudes. These coronal regions are away from the HCS and streamers. There are no closed-loop systems at these latitudes to trap the solar plasma, which might escape as the slow wind.

Thus, the origins of the fast and slow solar wind are known, as also their strong associations with CHs and active regions on the sun. However, their generation mechanisms are yet to be convincingly established.

5.1. Some important unresolved problems :

- (i) The difference in the helium content between the slow wind around the heliomagnetic equator (helium-poor) and that (helium-rich) at high heliolatitudes during solar maximum.
- (ii) The peculiarities of the helium content in the solar wind *e.g.* very low values around sector boundaries, high variability in slow wind, constant value in HSS, very high values in several CMEs.
- (iii) If the fast and slow solar winds are of different nature, how can they maintain their separate identity knowing well that only the high-speed wind is markedly variable with the sunspot cycle?

5.2. Future scope :

It is suggested that the answers to such questions may lie in the source regions of the SW. However, these regions are too close to the sun to observe by any instrument [9]. These observations are possible only if the SOHO (Solar and Heliospheric Observatory) carries a new class of appropriate instruments on board when it will be launched in mid-1995, 1.5×10^6 km sunward from the earth. One of the primary aims of the SOHO mission is the understanding of the processes that heat and maintain the solar corona and generate the solar wind.

Acknowledgment

I sincerely thank Prof R K Varma for suggesting to publish this overview and also for supporting this work. I highly appreciate Mr D Stephen's efficient typing of this manuscript. This work was done under the CSIR Emeritus Scientist Scheme No. 21 (260)/92-EMR-II.

References

- [1] A J Dessler *Rev. Geophys.* **5** 1 (1967)
- [2] A S Krieger, A F Timothy and E C Roelof *Solar Phys.* **23** 123 (1973)
- [3] W M Neupert and V Pizzo *J. Geophys. Res.* **79** 3701 (1974)
- [4] J T Nolte, A S Krieger, A F Timothy, R E Gold, E C Roelof, G S Vaiana, A J Lazarus, J D Sullivan and P S McIntosh *Solar Phys.* **46** 303 (1976)
- [5] A F Timothy, A S Krieger and G S Vaiana *Solar Phys.* **42** 135 (1975)
- [6] W C Feldman, J R Asbridge, S J Bame and J T Gosling *Geophys. Res.* **81** 5054 (1976)
- [7] W C Feldman, J R Asbridge, S J Bame and J T Gosling *J. Geophys. Res.* **83** 2177 (1978)
- [8] W C Feldman, J R Asbridge, S J Bame and J T Gosling *J. Geophys. Res.* **83** 5285 (1978)
- [9] R Schwenn *Phys. Inner Heliosphere 1* eds. R Schwenn and E Marsch (Berlin : Springer-Verlag) (1990)
- [10] M Kojima and T Kakinuma *Space Sci. Rev.* **53** 273 (1990)
- [11] B J Rickett and W A Coles *J. Geophys. Res.* **96** 1717 (1991)
- [12] S K Alurkar, P Janardhan and H O Vats *Solar Phys.* **144** 385 (1993)
- [13] A J Hundhausen, R T Hansen and S F Hansen *J. Geophys. Res.* **86** 2079 (1981)
- [14] J T Hoeksema, J M Wilcox and P H Scherrer *J. Geophys. Res.* **87** 10331 (1982)
- [15] J T Hoeksema, J M Wilcox and P H Scherrer *J. Geophys. Res.* **88** 9910 (1983)
- [16] G L Withbroe *Astrophys. J.* **325** 422 (1988)
- [17] E N Parker *COSPAR Collo. Series Vol. 3 Solar Wind Seven* eds. E Marsch and R Schwenn (1992)
- [18] M Neugebauer *COSPAR Collo. Series Vol. 3 Solar Wind Seven* eds. E Marsch and R Schwenn (1992)
- [19] W I Axford and J F McKenzie *COSPAR Collo. Series Vol. 3 Solar Wind Seven* eds. E Marsch and R Schwenn (1992)
- [20] E Leer *Proc. Sixth Int. Solar Wind Conf. Vol. I* eds. V J Pizzo, T E Holzer and D G Sime (1988)
- [21] J V Hollweg *Solar Phys.* **56** 305 (1978)
- [22] J V Hollweg *Solar Phys.* **70** 25 (1981)
- [23] E Leer, T E Holzer and T Fla *Space Sci. Rev.* **33** 161 (1982)
- [24] T Fla, S R Habbal, T E Holzer and E Leer *Astrophys. J.* **280** 382 (1984)
- [25] G W Pneuman and F Q Orrall *Physics of the Sun Vol. II* eds. P A Sturrock *et al* (Dordrecht : D Reidel) p 71 (1986)
- [26] M K Bird and P Edenhofer *Phys. Inner Heliosphere 1* eds. R Schwenn and E March (Berlin : Springer-Verlag) (1990)
- [27] G E Brueckner and D F Bartoe *Astrophys. J.* **272** 329 (1983)
- [28] R A Howard and M J Koomen *Solar Phys.* **37** 469 (1974)
- [29] J B Zirkar *Rev. Geophys. Space Phys.* **15** 257 (1977)
- [30] J T Nolte, A S Krieger, E C Roelof and R E Gold *Solar Phys.* **51** 459 (1977)
- [31] L Svalgaard and J M Wilcox *Ann. Rev. Astron. Astrophys.* **16** 429
- [32] G L Withbroe, J L Kohl, H Weiser and R H Munro *Astrophys. J.* **297** 324 (1985)
- [33] B J Rickett and W A Coles *Solar Wind 5* ed. M Neugebauer NASA CP-2280 315 (1983)
- [34] R H Levine, M D Altschuler and J W Harvey *J. Geophys. Res.* **82** 1061 (1977)

- [35] M D Altschuler and G Newkirk (Jr.) *Solar Phys.* **9** 131 (1969)
- [36] B A Lindblad *Astrophys. Space Sci.* **170** 55 (1990)
- [37] A J Hundhausen *Coronal Holes and High Speed Solar Wind Streams* ed. J B Zirker (Boulder-Colorado : Associated Press) p 255 (1977)
- [38] M Dryer *Space Sci. Rev.* **33** 233 (1982)
- [39] E Hildner *Adv. Space Res.* **6** 297 (1986)
- [40] R A Howard, N R Sheeley, D J Michels and M J Koomen *The Sun and the Heliosphere in Three Dimensions* ed. R G Marsden 107 (1986)
- [41] W J Wagner *Ann. Rev. Astron. Astrophys.* **22** 267 (1984)
- [42] A J Hundhausen *Proc. Sixth Int. Solar Wind Conf. Vol. I* eds. V J Pizzo, T E Holzer and D G Sime (1988)
- [43] J T Gosling, E Hildner, R M MacQueen, R H Munro, A I Poland and C L Ross *J. Geophys. Res.* **79** 4581 (1974)
- [44] R H Munro, J T Gosling, E Hildner, R M MacQueen, A I Poland and C L Ross *Solar Phys.* **61** 201 (1979)
- [45] D F Webb, A S Krieger and D M Rust *Solar Phys.* **48** 159 (1976)
- [46] S Kahler *Astrophys. J.* **214** 891 (1977)
- [47] A J Hundhausen, T E Holzer and B C Low *J. Geophys. Res.* **92** 173 (1987)
- [48] N R Sheeley (Jr.), R A Howard, M J Koomen, D J Michels, R Schwenn, K H Muhlhauser and H Rosenbauer *J. Geophys. Res.* **90** 163 (1985)
- [49] G L Withbroe *The Sun and the Heliosphere in Three Dimensions* ed. R G Marsden (1986)
- [50] J T Gosling, G Borrini, J R Asbridge, S J Bame, W C Feldman and R T Hansen *J. Geophys. Res.* **86** 5438 (1981)
- [51] I A Ahmad and G L Withbroe *Solar Phys.* **53** 397 (1977)
- [52] G J Rottman, F Q Orrall and J A Klimchuck *Astrophys. J. Lett.* **247** L135 (1981)
- [53] G L Withbroe, J L Hohl, H Weiser, G Noli and R H Munro *Astrophys. J.* **254** 361 (1982)
- [54] R D Ekers and L T Little *Astron. Astrophys.* **10** 310 (1971)
- [55] J W Armstrong and R Woo *Astron. Astrophys.* **103** 415 (1981)
- [56] G L Tyler, J Y Vesecky, M A Plume, M T Howard and A Barness *Astrophys. J.* **249** 318 (1981)
- [57] E N Parker *Astrophys. J.* **128** 664 (1958)
- [58] E N Parker *Interplanetary Dynamical Processes* (New York : Interscience) (1963)
- [59] A Hewish, S J Tappin and G R Gapper *Nature* **314** 137 (1985)
- [60] M K Bird *Space Sci. Rev.* **33** 99 (1982)
- [61] R Woo *Astrophys. J.* **219** 727 (1978)
- [62] G L Tyler, J P Brenkle, T A Komarek and A J Zygbeun *J. Geophys. Res.* **82** 4345 (1977)
- [63] R Woo, F C Yang and A Ishimaru *Astrophys. J.* **218** 557 (1977)
- [64] N A Armand, A I Efimov and O I Yokovlev *Astron. Astrophys.* **183** 135 (1987)
- [65] N A Lotova *Solar Phys.* **117** 399 (1988)
- [66] S L Scott, W A Coles and G Bourgois *Astron. Astrophys.* **123** 207 (1983)
- [67] D F Blum and N A Lotova *Geomagnetizm i Aeronomiya* **23** 361 (1983)

- [68] D F Blum, N A Lotova and R L Sorochenko *Geomagnetizm i Aeronomiya* **24** 537 (1984)
- [69] P A Dennison and R G Blessing *Proc. Astron. Soc. Australia* **2** 86 (1972)
- [70] G J Rottman and F Q Orrall *Solar Wind* 5 ed. M Neugebauer NASA CP-2280 (1983)
- [71] M Kojima, J W Armstrong, W A Coles and B J Rickett *Proc. Sixth Int. Solar Wind Conf. Vol. I* ed. V J Pizzo, T E Holzer, D G Sime (1987)
- [72] W A Coles *Space Sci. Rev.* **21** 44 (1978)
- [73] T E Holzer *Solar System Plasma Phys.* **103** 103 (1979)
- [74] T E Holzer and E Leer *J. Geophys. Res.* **85** 4665 (1980)
- [75] E Leer and T E Holzer *J. Geophys. Res.* **85** 4681 (1980)
- [76] J V Hollweg *Rev. Geophys.* **16** 689 (1978)
- [77] R H Munro and B V Jackson *Astrophys. J.* **213** 874 (1977)
- [78] E N Parker *Astrophys. J.* **372** 719 (1991)
- [79] J W Belcher and L Davis *J. Geophys. Res.* **76** 3534 (1971)
- [80] G Borrini, J T Gosling, S J Bame and W C Feldman *Solar Phys* **83** 367 (1983)
- [81] R Schwenn *Adv. Space Res.* **1** 3 (1981)
- [82] O I Yokovlev, A I Efimov, V M Ruzmanov and V K Shtrykov *Astron. Zh.* **57** 790 (1980)

About the Reviewer

S K Alurkar

Professor S K Alurkar started his research career under the supervision of the late Professor K R Ramanathan at the Physical Research Laboratory, Ahmedabad. After earning a Ph.D. in "Physics of the lower ionosphere" in 1965, he switched over to Solar Radio Astronomy wherein he was responsible for developing a number of Radio Astronomy instruments for studying solar radio emissions over a decade, resulting in several new findings.

These studies were extended to the interplanetary medium, first under a DST-sponsored project followed by an Indo-US collaborative project. For this, a three-telescope system, with large antenna arrays, was deployed at Thaltej (Ahmedabad), Rajkot and Surat to study the solar wind velocity structure using the well-known IPS technique. The largest telescope at Thaltej also enabled us to study the density structure of cometary plasma tails as they caused IPS of radio galaxies. These were the first ever findings which were presented in international meetings and also published in reputed journals.

Dr Alurkar is now working at PRL as an Emeritus Scientist (CSIR).